Chapter 7: Free Shear Flows: Jets, Mixing Layers and Wakes (Pope)

Part 2: Plane Mixing Layer and Plain Wake

Plane Mixing layer

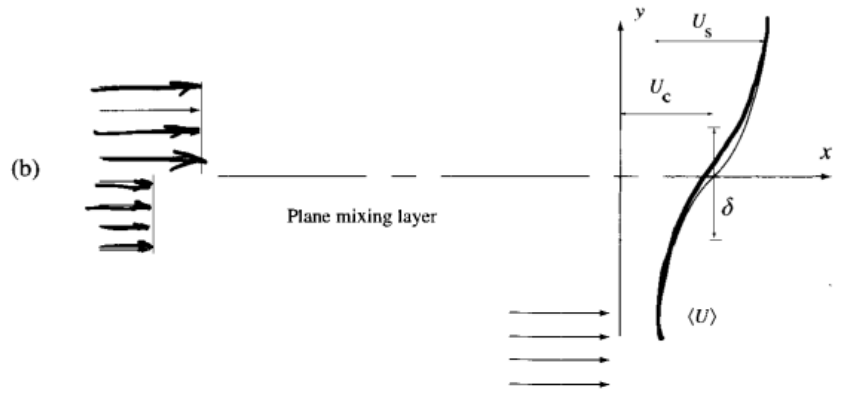

The flow depends on two characteristic velocities U_h and U_l: U_l/U_h.

$$U_c \equiv \frac{1}{2}(U_h + U_l) = \text{convection velocity}$$

$$U_s \equiv U_h - U_l = \text{velocity difference}$$

U_h, U_l, U_c, and U_s are constant, independent of x.

Mean velocity profile:

$$\langle U(x,y)\rangle \neq f(z)$$

$x =$ direction flow, $y =$ crossflow direction, and $z =$ spanwise direction.

$\delta(x) =$ characteristic width

For $0 < \alpha < 1$, define cross-stream location $y_a(x)$ such that:

$$\langle U(x, y_a(x), 0)\rangle = U_l + \alpha(U_h + U_l)$$

And take $\delta(x)$ to be:

$$\delta(x) = y_{0.9}(x) - y_{0.1}(x)$$

In addition, reference lateral position $\overline{y}(x)$:

$$\overline{y}(x) = \frac{1}{2}[y_{0.9}(x) + y_{0.1}(x)]$$

Scaled cross-stream coordinate:

$$\xi = \frac{[y - \overline{y}(x)]}{\delta(x)}$$

Scaled velocity:

$$f(\xi) = \frac{(\langle U \rangle - U_c)}{U_s}$$

Where $f(\pm\infty) = \pm 1/2$ and $f(\pm 1/2) = \pm 0.4$

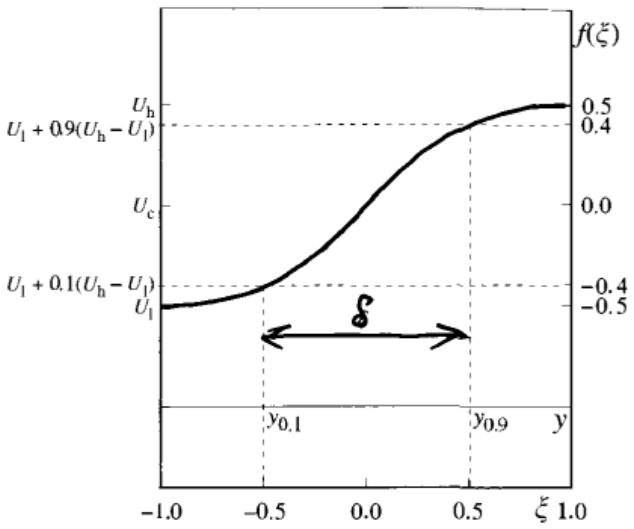

Fig. 5.21. A sketch of the mean velocity $\langle U \rangle$ against y, and of the scaled mean velocity profile $f(\xi)$, showing the definitions of $y_{0.1}$, $y_{0.9}$, and δ.

$$f(+\infty) = U_h - \frac{1}{2}U_h - \frac{1}{2}U_l \rightarrow \frac{1}{2}\frac{(U_h - U_l)}{U_s} = \frac{1}{2}$$

$$f(-\infty) = U_l - \frac{1}{2}U_h - \frac{1}{2}U_l \rightarrow -\frac{1}{2}\frac{(U_h - U_l)}{U_s} = -\frac{1}{2}$$

For $U_l/U_h = 0$, i.e., $U_l = 0$: EFD confirms self-similarity $\langle U \rangle$ and $\langle u_i u_j \rangle$ and the mixing layers spreads linearly.

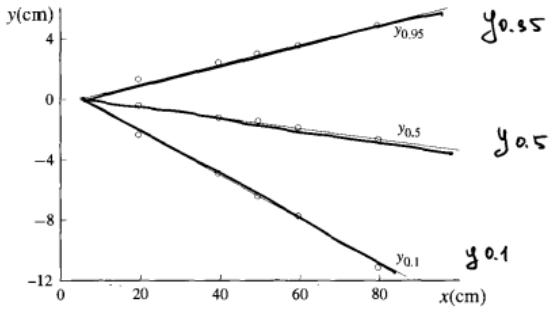

Fig. 5.23. Axial variations of $y_{0.1}$, $y_{0.5}$, and $y_{0.95}$ in the plane mixing layer, showing the linear spreading. Experimental data of Champagne *et al.* (1976).

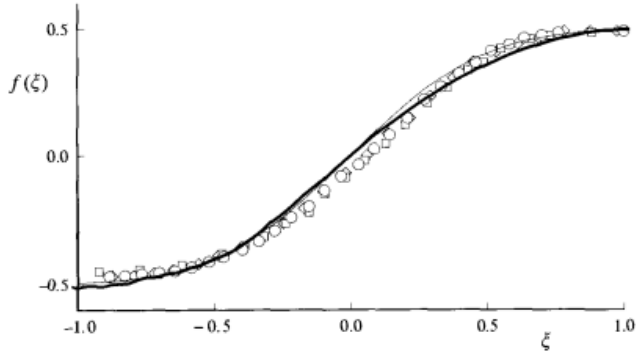

Fig. 5.22. Scaled velocity profiles in a plane mixing layer. Symbols, experimental data of Champagne *et al.* (1976) (◇, x = 39.5 cm; □, x = 49.5 cm; ○, x = 59.5 cm); line, error-function profile (Eq. (5.224)) shown for reference.

Flow not symmetric about y or $\xi = 0$.

High speed spreads into low-speed stream.

Linear spreading as with round and plane jet, consequence of self-similarity.

Self-similarity form of BL equation (Pope Ex. 5.29-5.34, including temporal mixing layer):

$$\underbrace{\left(\frac{U_c}{U_s}\frac{d\delta}{dx}\right)}_{\boxed{S}}\left(\xi + \frac{U_s}{U_c}\int_0^{\xi} f(\xi)d\xi\right)f' = g'$$

$S = \text{constant} \neq f(x)$ as required and already noted $\delta = Sx$.

To an observer travelling in the x direction at U_c, the fractional growth rate of the mixing layer is $U_c\, d\ln\delta\,/dx$. Normalized by the local timescale δ/U_s, resulting non-dimensional parameter is:

$$\frac{\delta}{U_s}U_c\frac{d\ln\delta}{dx}=\frac{U_c}{U_s}\frac{d\delta}{dx}=S$$

$$S\neq f(U_l/U_h)\therefore\frac{d\delta}{dx}\propto\frac{U_s}{U_c}$$

$$0.06\leq S\leq 0.11$$

In the limit case: $U_s/U_c\to 0$, i.e., $U_l/U_h\to 1$

$$U_c\equiv\frac{1}{2}(U_h+U_l)=\text{convection velocity}$$

$$U_s\equiv U_h-U_l=\text{velocity difference}$$

$$\frac{U_s}{U_c}=\frac{(U_h-U_l)}{\frac{1}{2}(U_h+U_l)}\to 0\ \Rightarrow U_h=U_l\to\frac{U_l}{U_h}=1$$

BL equation becomes:

$$U_c\frac{\partial\langle U\rangle}{\partial x}=-\frac{\partial\langle uv\rangle}{\partial y}$$

An observer travelling at speed U_c sees the two streams $(y\to\infty\text{ and }y\to-\infty)$ moving to the right and left, with velocities $0.5U_s$ and $-0.5U_s$, respectively.

$$\frac{\partial}{\partial x}\sim\frac{U_s}{U_c}\to\frac{\partial}{\partial y}\gg\frac{\partial}{\partial x}$$

$$\delta(t)\sim SU_s$$

As $U_s/U_c \to 0$, the flow becomes statistically 1D, $f(t)$, and symmetric about y = 0 → temporal mixing layer.

DNS: self-similar → $\delta(t) \propto t,\ S \approx 0.062.$

EFD $U_l/U_h = 0.6$ spatial mixing layer, $S = 0.069.$

EFD, DNS, and $\nu_t =$ constant BL solution good agreement, except outer flow merging with free stream velocities.

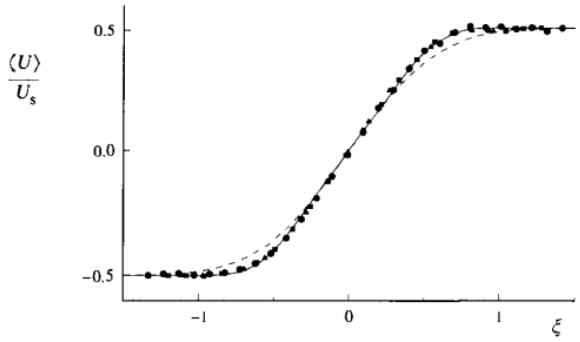

Fig. 5.24. The scaled mean velocity profile in self-similar plane mixing layers. Symbols, experiment of Bell and Mehta (1990) ($U_l/U_h = 0.6$); solid line, DNS data for the temporal mixing layer (Rogers and Moser 1994); dashed line, error-function profile with width chosen to match data in the center of the layer.

Longo, J., Huang, H.P., and Stern, F., "Solid-Fluid Juncture Boundary Layer and Wake," Experiments in Fluids, Vol. 25, No. 4, September 1998, pp. 283 – 297.

Sreedhar, M. and Stern, F., "Prediction of Solid/Free-Surface Juncture Boundary Layer and Wake of a Surface-Piercing Flat Plate at Low Froude Number," ASME J. Fluids Eng., Vol. 120, June 1998, pp. 354 – 362.

Sreedhar, M. and Stern, F., "Large Eddy Simulation of Temporally Developing Juncture Flows," Int. J. Num. Meth. Fluids, Vol. 28, No. 1, 15 July 1998, pp. 47 – 72

For mixing layer, since $U_s \equiv U_h - U_l =$ fixed and $\delta(t) \propto x$, $\mathrm{Re}_0(x)=U_s\delta/\nu$ and ν_t also $\propto x$.

$$\dot{K}(x) = \int_{-\infty}^{\infty} \langle U \rangle k dy$$

Represents TKE flux and scales as $U_c U_s^2 \delta$, i.e., $\propto x$.

In jets and wakes, $\dot{K}(x)$ decreases with x.

Because $\dot{K}(x) \propto x$, averaged across flow P > ε, e.g., in the center of the layer $P/\varepsilon \sim 1.4$.

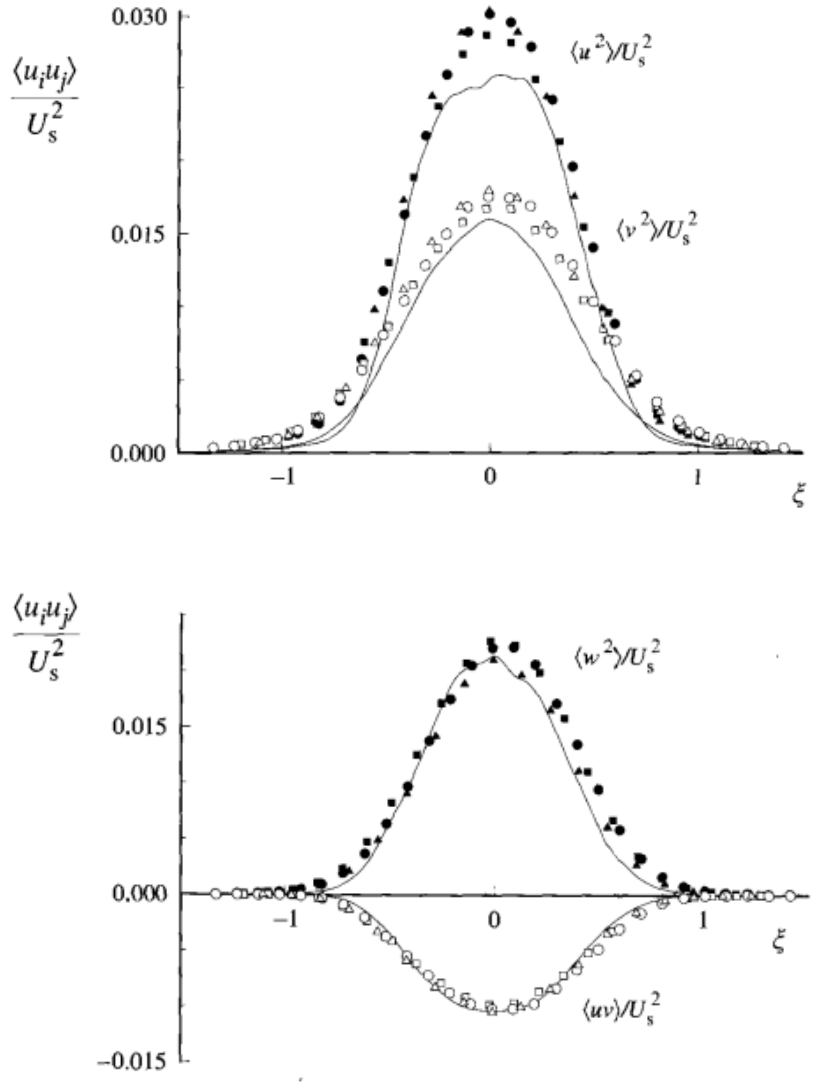

Fig. 5.25. Scaled Reynolds-stress profiles in self-similar plane mixing layers. Symbols, experiment of Bell and Mehta (1990) ($U_l/U_h = 0.6$); solid line, DNS data for the temporal mixing layer (Rogers and Moser 1994).

Shows some differences temporal vs spatial mixing layer.

Plane Wake

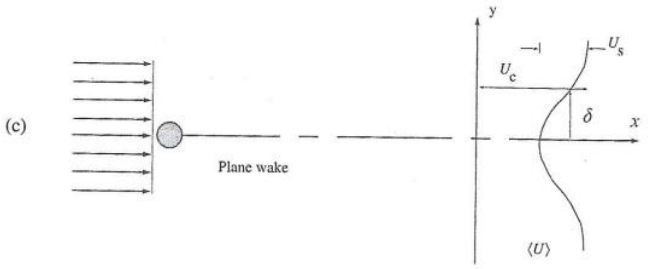

Statistically stationary (steady), 2D and symmetric about the plane $y = 0$.

Characteristic velocities:

$U_c =$ free stream velocity

$U_s =$ velocity difference $\rightarrow U_s(x) = U_c - \overline{U}(x, 0) =$ centerline velocity deficit.

Half width:

$$\overline{U}\left(x, \pm y_{1/2}, 0\right) = U_c - \frac{1}{2} U_s(x)$$

As the wake develops, $y_{1/2}$ increases and $U_s/U_c \rightarrow 0$

In the mixing layer $U_s/U_c =$ constant $\neq f(x)$, whereas in the wake $U_s/U_c = f(x)$
$\therefore$ flow not exactly self-similar, only asymptotically self-similar as $U_s/U_c \rightarrow 0$, i.e., < 0.1.

Using the cross-stream similarity variable $\xi = y/y_{1/2}$, the self-similar velocity defect $f(\xi)$ is:

$$f(\xi) = \frac{U_c - \overline{U}(x, y, 0)}{U_s(x)}$$

So that the mean velocity is:

$$\overline{U} = U_c - U_s(x)\, f(\xi) \quad (1)$$

Using these definitions, $f(0) = 1$ and $f(\pm 1) = 1/2$.

Momentum deficit flow rate per unit span:

$$\dot{M}(x) = \int_{-\infty}^{\infty} \rho \overline{U}\left(U_c - \overline{U}\right) dy$$

$$= \rho U_c U_s(x) y_1(x) \int_{-\infty}^{\infty} \left(1 - \frac{U_s}{U_c} f(\xi)\right) f(\xi) d\xi \neq f(x)$$

Equal to the body drag / span width.

$$\therefore U_s(x) y_{1/2}(x) \neq f(x)$$

Derivation: BL momentum equation neglecting viscosity term:

$$\overline{U}\frac{\partial \overline{U}}{\partial x} + \overline{V}\frac{\partial \overline{U}}{\partial y} = -\frac{\partial \overline{uv}}{\partial y} \quad (2)$$

For wakes and jets:

$$\left(\overline{U} - U_c\right) \underbrace{\left(\frac{\partial \overline{U}}{\partial x} + \frac{\partial \overline{V}}{\partial y}\right)}_{\boxed{\text{continuity}}} = 0 \quad (3)$$

And since U_c = constant,

$$\overline{U}\frac{\partial U_c}{\partial x} + \overline{V}\frac{\partial U_c}{\partial y} = 0 \quad (4)$$

Adding Eq. (2) and (3) and subtracting Eq. (4) gives:

$$\frac{\partial}{\partial x}\left[\overline{U}\left(U_c - \overline{U}\right)\right] + \frac{\partial}{\partial y}\left[\overline{V}\left(U_c - \overline{U}\right)\right] = \frac{\partial}{\partial y}\overline{uv} \quad (5)$$

$\overline{U} - U_c$ and $\overline{uv} \to 0$ for $|y| \to \infty$. Thus, Eq, (5) can be integrated across the flow:

$$\frac{d}{dx}\int_{-\infty}^{\infty}\overline{U}\left(U_c - \overline{U}\right)dy = 0$$

Thus, total mean flux of momentum per unit length in spanwise direction is:

$$\dot{M} = \rho\int_{-\infty}^{\infty}\overline{U}\left(U_c - \overline{U}\right)dy = \text{constant} \neq f(x)$$

Recall Eq. (1):

$$\overline{U} = U_c - \underbrace{U_s(x)\, f(\xi)}_{\boxed{\text{velocity deficit}}}$$

For the similarity variable:

$$\xi = \frac{y}{y_{1/2}(x)}$$

$$\frac{d\xi}{dx} = -\frac{y}{y_{1/2}^2}\frac{dy_{1/2}}{dx} = -\frac{\xi}{y_{1/2}}\frac{dy_{1/2}}{dx}$$

$$\frac{d\xi}{dy} = \frac{1}{y_{1/2}(x)}$$

Substituting Eq. (1) into Eq. (2):

$$\left(U_c - U_s(x)\, f(\xi)\right)\frac{\partial \overline{U}}{\partial x} + \overline{V}\frac{\partial \overline{U}}{\partial y} = -\frac{\partial \overline{uv}}{\partial y} \qquad (6)$$

For the shear stress:

$$\overline{uv} = U_s^2 g(\xi)$$

$$\frac{\partial \overline{uv}}{\partial y} = U_s^2 \frac{\partial g(\xi)}{\partial \xi}\frac{\partial \xi}{\partial y} = \frac{U_s^2}{y_{1/2}}\frac{\partial g(\xi)}{\partial \xi}$$

The mean velocity gradients can be expressed as:

$$\frac{\partial \overline{U}}{\partial x} = \cancel{\frac{\partial U_c}{\partial x}} - \frac{\partial U_s(x)}{\partial x} f(\xi) - U_s \frac{\partial f(\xi)}{\partial \xi}\frac{\partial \xi}{\partial x} = -\frac{\partial U_s}{\partial x} f(\xi) + U_s f' \frac{\xi}{y_{1/2}}\frac{dy_{1/2}}{dx}$$

$$\frac{\partial \overline{U}}{\partial y} = \cancel{\frac{\partial U_c}{\partial y}} - \cancel{\frac{\partial U_s(x)}{\partial y} f(\xi)} - U_s \frac{\partial f(\xi)}{\partial \xi}\frac{\partial \xi}{\partial y} = -\frac{U_s f'}{y_{1/2}}$$

$$\frac{\partial \overline{V}}{\partial y} = -\frac{\partial \overline{U}}{\partial x} \rightarrow \overline{V} = -\frac{\partial \overline{U}}{\partial x} y_{1/2}\, \xi$$

Consequently, the term $\overline{V}\frac{\partial \overline{U}}{\partial y}$ in Eq. (6) is equal to:

$$\overline{V}\frac{\partial \overline{U}}{\partial y} = -y_{1/2}\, \xi \frac{\partial \overline{U}}{\partial x}\frac{\partial \overline{U}}{\partial y}$$

And it is negligible, since $\overline{U}_x \overline{U}_y$ is small (BL).

Consequently, Eq. (6) becomes:

$$\left(U_c - U_s(x)\, f(\xi)\right)\frac{\partial \overline{U}}{\partial x} = -\frac{\partial \overline{uv}}{\partial y} \quad (7)$$

And in the far wake,

$$U_s(x)\, f(\xi) \ll U_c$$

Such that, the BL equation becomes:

$$U_c \frac{\partial \overline{U}}{\partial x} = -\frac{\partial \overline{uv}}{\partial y} \quad (8)$$

Rewriting this equation with the aid of the mean velocity gradients expressions obtained previously gives:

$$U_c\left(-\frac{\partial U_s}{\partial x}\, f(\xi) + U_s f' \frac{\xi}{y_{1/2}}\frac{dy_{1/2}}{dx}\right) = -\frac{U_s^2}{y_{1/2}}\frac{\partial g(\xi)}{\partial \xi}$$

$$-U_c \frac{\partial U_s}{\partial x}\, f(\xi) + U_c U_s f' \frac{\xi}{y_{1/2}}\frac{dy_{1/2}}{dx} = -\frac{U_s^2}{y_{1/2}}\frac{\partial g(\xi)}{\partial \xi} \quad (9)$$

Recall:

$$U_s(x) y_{1/2}(x) \neq f(x) = \text{constant}$$

Such that:

$$\frac{dU_s}{dx} y_{1/2} + U_s \frac{dy_{1/2}}{dx} = 0 \rightarrow \frac{dU_s}{dx} = -\frac{U_s}{y_{1/2}}\frac{dy_{1/2}}{dx} \quad (10)$$

Define the spreading parameter:

$$S \equiv \frac{U_c}{U_s}\frac{dy_{1/2}}{dx} \quad (11)$$

And substituting Eqs. (10) and (11) into Eq. (9) gives:

$$-U_c\left(-\frac{U_s}{y_{1/2}}\frac{dy_{1/2}}{dx}\right) f(\xi) + U_c U_s f' \frac{\xi}{y_{1/2}}\frac{dy_{1/2}}{dx} = -\frac{U_s^2}{y_{1/2}}\frac{\partial g(\xi)}{\partial \xi}$$

$$U_c \frac{U_s}{y_{1/2}}\frac{dy_{1/2}}{dx} f(\xi) + U_c U_s f' \frac{\xi}{y_{1/2}}\frac{dy_{1/2}}{dx} = -\frac{U_s^2}{y_{1/2}}\frac{\partial g(\xi)}{\partial \xi} \quad (12)$$

Multiplying Eq. (12) by $y_{1/2}/U_s^2$ gives:

$$\underbrace{\frac{U_c}{U_s}\frac{dy_{1/2}}{dx}}_{\boxed{S}} f(\xi) + \underbrace{\frac{U_c}{U_s}\frac{dy_{1/2}}{dx}}_{\boxed{S}} f'\xi = -\frac{\partial g(\xi)}{\partial \xi}$$

$$\underbrace{S\, f(\xi) + \xi S f'(\xi)}_{\boxed{S(\xi f)'}} = -g'(\xi)$$

$$S(\xi f)' = -g'(\xi) \quad (13)$$

Variation of quantities with x:

$$U_s(x)y_{1/2}(x) = \text{constant, i.e., S = constant}$$

$$y_{1/2}(x) \sim x^{1/2}$$

$$\frac{dy_{1/2}}{dx} \sim \frac{1}{2}x^{-1/2}$$

$$\frac{dU_s}{dx} \sim -\frac{1}{2}x^{-3/2}$$

Integrating Eq. (13):

$$g = -S\,\xi f = \frac{\overline{uv}}{U_s^2}$$

Assuming constant turbulent viscosity:

$$\nu_t = \hat{\nu}_t U_s(x)y_{1/2}(x) \neq f(x)$$

The shear stress is given by:

$$\overline{uv} = -\nu_t \frac{\partial \overline{U}}{\partial y} = \nu_t \frac{U_s f'}{y_{1/2}} = U_s^2 g$$

And isolating g:

$$g = \frac{\nu_t f'}{U_s y_{1/2}} = \hat{\nu}_t f' = -S\,\xi f$$

Which gives an equation for f:

$$f' = -\frac{S\xi}{\hat{\nu}_t} f$$

$$\frac{df}{f} = -\frac{S\xi}{\hat{\nu}_t} d\xi \rightarrow \ln f = -\frac{S\xi^2}{2\hat{\nu}_t} + C$$

$$f = C \exp\left(-\frac{S\xi^2}{2\hat{\nu}_t}\right)$$

Taking

$$\alpha = \frac{S}{2\hat{\nu}_t}$$

The solution becomes:

$$f(\xi) = C \exp(-\alpha\xi^2)$$

With BCs $f(0) = 1$ and $f(\pm 1) = 1/2$:

$$f(0) = C = 1$$
$$f(1) = \exp(-\alpha) = \frac{1}{2} \rightarrow \alpha = \ln 2$$

Therefore, the final solution is:

$$f(\xi) = \exp(-\ln 2\, \xi^2)$$

And

$$\ln 2 = \frac{S}{2\hat{\nu}_t} \rightarrow \frac{1}{\hat{\nu}_t} = \frac{2 \ln 2}{S} = R_T$$

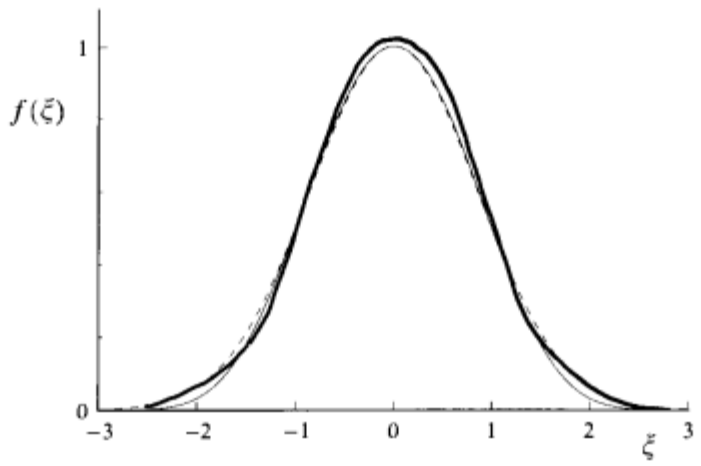

Fig. 5.26. The normalized velocity defect profile in the self-similar plane wake. Solid line, from experimental data of Wygnanski *et al.* (1986); dashed line, constant-turbulent-viscosity solution, Eq. (5.240).

Data from circular cylinder, symmetric foil, and thin rectangular plate: $S = 0.093, 0.103$, and 0.075, respectively.

$$g = \frac{\overline{uv}}{U_s^2} = -S\xi f$$

$$\frac{\langle u^2 \rangle_{max}^{1/2}}{U_s} = 0.32 \text{ plate}$$

$$= 0.41 \text{ airfoil}$$

Conclusion: self-similarity achieved, albeit retaining effects from IC.

Show that $\alpha = \ln 2$, and hence that

$$\frac{1}{\hat{\nu}_T} = \frac{2 \ln 2}{S}. \tag{5.252}$$

5.4.4 *The axisymmetric wake*

The analysis of the axisymmetric wake parallels closely that of the plane wake. However, the experimental data reveal striking differences.

An axisymmetric wake forms behind a round object – a sphere, spheroid, or disk, for example – held in a uniform stream, flowing with velocity U_c in the x direction. The flow is statistically axisymmetric, with statistics depending on x and r, but being independent of θ. The centerline velocity deficit $U_s(x)$ and flow half-width $r_{1/2}(x)$ are defined in the obvious manner.

Just as with the plane wake, self-similarity is possible only as U_s/U_c tends to zero, and then the spreading parameter $S = (U_c/U_s)\,\mathrm{d}r_{1/2}/\mathrm{d}x$ is constant. For this flow, however, the momentum deficit flow rate – which equals the drag on the body – is proportional to $\rho U_c U_s r_{1/2}^2$. As a consequence U_s varies as $x^{-2/3}$ and $r_{1/2}$ as $x^{1/3}$, so that the Reynolds number decreases as $x^{-1/3}$. The assumption that the turbulent viscosity is uniform across the flow leads to the same mean velocity-deficit profile as that for the plane wake (Eqs. (5.239)–(5.241)).

Uberoi and Freymuth (1970) reported measurements made in the wake of a sphere (of diameter d), with Reynolds number $\mathrm{Re}_d \equiv U_c d/\nu = 8,600$. After a development distance ($x/d < 50$), self-similarity in the mean velocity and Reynolds stresses is observed over the range of x/d examined ($50 < x/d < 150$). The measured mean velocity-deficit profile is compared with the constant-turbulent-viscosity solution in Fig. 5.27, and the profiles of r.m.s. velocities are shown in Fig. 5.28. It should be observed that the peak value of $\langle u^2 \rangle^{1/2}/U_s$ is about 0.9, much higher than those in the other flows we have examined. Correspondingly, the spreading parameter is $S \approx 0.51$ – at least five times larger than that observed in plane wakes.

The balance of the turbulent kinetic energy (Fig. 5.29) is also substantially different than those of other flows. The dominant term is convection from upstream (i.e., $-\langle U \rangle\, \partial k/\partial x$), with dissipation ε and lateral transport each being about half as large. In contrast, at its peak, the production $\mathcal{P}$ is just 20% of ε, and 15% of convection. The dominance of convection, and the relatively small amount of production, suggest that the turbulence is strongly influenced by conditions upstream.

This hypothesis is strengthened by the observation that the measured

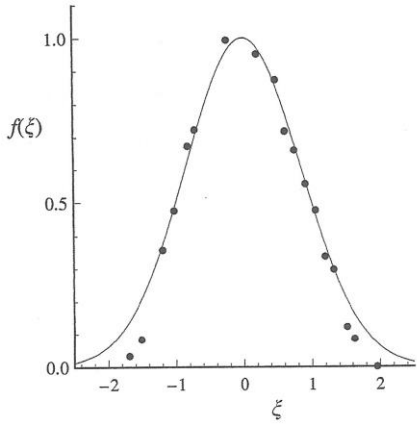

Fig. 5.27. Mean velocity-deficit profiles in a self-similar axisymmetric wake. Symbols, experimental data of Uberoi and Freymuth (1970); line, constant-turbulent-viscosity solution $f(\xi) = \exp(-\xi^2 \ln 2)$.

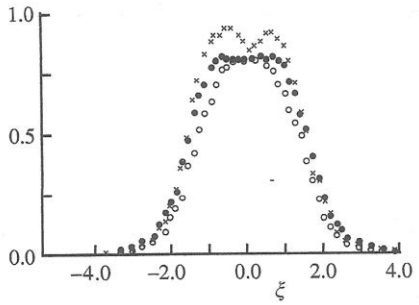

Fig. 5.28. R.m.s. velocity profiles in a self-similar axisymmetric wake. Experimental data of Uberoi and Freymuth (1970): ×, $\langle u^2 \rangle^{1/2}/U_s$; •, $\langle v^2 \rangle^{1/2}/U_s$; ○, $\langle w^2 \rangle^{1/2}/U_s$.

spreading parameter and turbulence level depend very significantly on the geometry of the body that generates the wake (see Table 5.3). On going from streamlined bodies to bluff bodies, S increases by a factor of ten, and the relative turbulence intensity by a factor of three. These observations are discussed further in Section 5.5.4.

Of the free shear flows examined in this chapter, only in the axisymmetric wake does the Reynolds number decrease with x (as $x^{-1/3}$). Consequently,

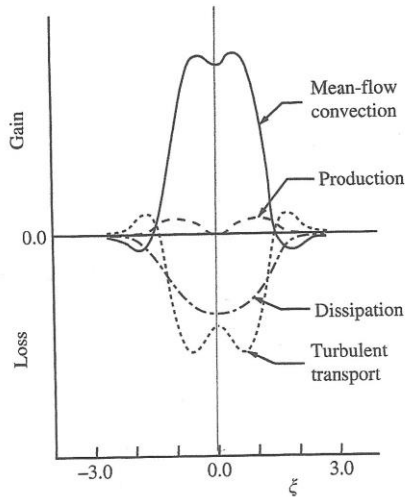

Fig. 5.29. The turbulent kinetic energy budget in a self-similar axisymmetric wake. Experimental data of Uberoi and Freymuth (1970).

Table 5.3. *The spreading parameter and turbulence intensity for axisymmetric wakes behind various bodies*

Body	Spreading parameter S	Turbulence intensity on centerline $\langle u^2\rangle_0^{1/2}/U_s$	Investigation
49% blockage-screen	0.064	0.3	Cannon and Champagne (1991)
6:1 spheroid	0.11	0.3	Chevray (1968)
84% blockage-screen	0.34	0.75	Cannon and Champagne (1991)
Sphere	0.51	0.84	Uberoi and Freymuth (1970)
Disk	0.71	1.1	Cannon and Champagne (1991)
Disk	0.8	0.94	Carmody (1964)

only over a limited range of x can self-similarity (independent of Re) be expected; for, at sufficiently large x, the flow can be assumed to relaminarizes. The laminar wake admits the same self-similar velocity profile, but with U_s and $r_{1/2}$ varying as x^{-1} and $x^{1/2}$, respectively. Some experimental data (e.g., Cannon and Champagne (1991)) suggest that modest departures from self-similarity (based on high-Reynolds-number scaling) occur.